

# Conditional Flow Variational Autoencoders for Structured Sequence Prediction

Apratim Bhattacharyya<sup>1</sup>, Michael Hanselmann<sup>2</sup>, Mario Fritz<sup>3</sup>, Bernt Schiele<sup>1</sup> and Christoph-Nikolas Straehle<sup>2</sup>

abhattac@mpi-inf.mpg.de, michael.hanselmann@de.bosch.com, fritz@cispa.saarland.de,  
schiele@mpi-inf.mpg.de, christoph-nikolas.straehle@de.bosch.com

<sup>1</sup>Max Planck Institute for Informatics, Saarland Informatics Campus, Saarbrücken, Germany

<sup>2</sup>Bosch Center for Artificial Intelligence, Renningen, Germany

<sup>3</sup>CISPA Helmholtz Center for Information Security, Saarland Informatics Campus, Saarbrücken, Germany

**Abstract:** Prediction of future states of the environment and interacting agents is a key competence required for autonomous agents to operate successfully in the real world. Prior work for structured sequence prediction based on latent variable models imposes a uni-modal standard Gaussian prior on the latent variables. This induces a strong model bias which makes it challenging to fully capture the multi-modality of the distribution of the future states. In this work, we introduce *Conditional Flow Variational Autoencoders* which uses our novel conditional normalizing flow based prior. We show that using our novel complex multi-modal conditional prior we can capture complex multi-modal conditional distributions. Furthermore, we study for the first time latent variable collapse with normalizing flows and propose solutions to prevent such failure cases. Our experiments on three multi-modal structured sequence prediction datasets – MNIST Sequences, Stanford Drone and HighD – show that the proposed method obtains state of art results across different evaluation metrics.

## 1 Introduction

Anticipating future states of the environment is a key competence necessary for the success of autonomous agents. In complex real world environments, the future is highly uncertain. Therefore, structured predictions, one to many mappings [1, 2] of the likely future states of the world, are important. In many scenarios, these tasks can be cast as sequence prediction problems. Particularly, conditional variational autoencoders (CVAE) [1] have been successful for such problems – from prediction of future pedestrians trajectories [3, 2, 4] to outcomes of robotic actions [5]. CVAEs model diverse futures by factorizing the distribution of future states using a set of latent variables which are mapped to likely future states. However, CVAEs assume a standard Gaussian prior on the latent variables which induces a strong model bias [6, 7] and makes it difficult for the model to capture multi-modal distributions. This can also cause latent variable collapse to the prior [8, 9, 10], where the latent variables do not encode useful information.

Recent work on (unconditional) variational autoencoders (VAE) has therefore focused on more complex priors e.g. Gaussian mixtures [7] and normalizing flows [11, 12]. While learning Gaussian mixture priors is difficult (e.g. determining the number of mixture components), normalizing flows enable the transformation of simple base densities e.g. standard Gaussians to complex multi-modal priors. However, since CVAEs have to deal with conditional distributions of varying complexity from uni-modal to highly multi-modal, directly integrating such priors with CVAEs is non trivial.

In this work, in order to model complex multi-modal conditional distributions, we propose *Conditional Flow Variational Autoencoders (CF-VAE)* with novel conditional normalizing flow based priors. In Figure 1, we show samples for MNIST handwriting stroke prediction. We observe that, given a starting stroke, our CF-VAE model with data dependent normalizing flow based latent prior captures the two main modes of the conditional distribution – i.e. 1 and 8 – while CVAEs with fixed uni-modal Gaussian prior predictions have limited diversity. Our contributions in this work are: 1. We propose Conditional Flow Variational Autoencoders with novel non-linear conditional normalizing flow based priors which can deal with conditional distributions of diverse complexities – uni-modal to highly

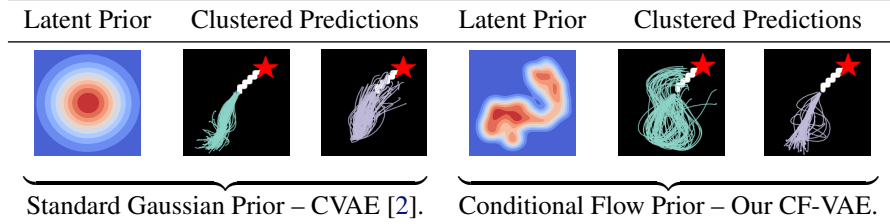


Figure 1: Clustered stroke predictions on MNIST sequences. Our Conditional Normalizing Flow based prior with two main modes enables our CF-VAE to capture the two main modes of the conditional distribution, while predictions with uni-modal Gaussian prior have limited diversity. Note, our 64D CF-VAE latent distribution is (approximately) projected to 2D using tSNE[13] and KDE[14].

multi-modal; 2. This is the first work to investigate latent variable collapse with normalizing flow based priors and to propose solutions to mitigate such collapse; 3. Finally, our method outperforms the previous state of the art on three important structured sequence prediction tasks – handwriting stroke prediction on MNIST, traffic participant trajectory prediction on Stanford Drone and vehicle trajectory prediction on HighD.

## 2 Related Work

**Normalizing Flows.** Normalizing flows are a powerful class of density estimation methods with exact inference. [15] introduced affine normalizing flows with triangular Jacobians. [16] extend flows with masked convolutions which allow for complex (non-autoregressive) dependence between the dimensions. In [17],  $1 \times 1$  convolutions were proposed with improved image generation compared to [16] and high resolution image synthesis. In [18] normalizing flows are auto-regressive and [19] extend it to ResNet. [20] extended normalizing flows to model conditional distributions. Here, we propose conditional normalizing flows to learn conditional priors for variational latent models.

**Variational Autoencoders.** The original variational autoencoder [21] used uni-modal Gaussian prior and posterior distributions. Thereafter, two lines of work have focused on developing either more complex prior or posterior distributions. In particular [22] proposes normalizing flows to model complex posterior distributions starting from a base Gaussian distribution. [23], introduced inverse autoregressive flows allowing more efficient sampling. In [24, 25] more complex householder and Sylvester normalizing flows were presented modeling even more complex posteriors. Here, we focus on orthogonal direction of more complex priors and thus the above approaches can be also integrated with our approach.

Recent work has also focused on learning more complex priors. In particular, [26] proposes a Dirichlet process prior and [27] proposes a nested Chinese restaurant process. However, these methods require sophisticated learning methods. In contrast, [7] proposes a mixture of Gaussians based prior (with fixed number of components) which is easier to train and shows promising results on some image generation tasks. [11], proposes a inverse autoregressive flow based prior which leads to improvements in complex image generation tasks like CIFAR-10. [12] proposes a prior for VAE based text generation using complex non-linear flows which allows for complex multi-modal priors. In contrast to these works, which learn unconditional priors, we aim to learn conditional priors to better capture multi-modal conditional distributions.

**Latent (Posterior) Collapse.** Latent or posterior collapse arises when the latent posterior does not encode any useful information. Most prior work [8, 28, 29, 30, 9] modifies the training objective, the KL divergence term between the prior and posterior is annealed. This enables more complex posteriors and prevents collapse to the prior. [31] extends KL annealing to CVAEs. However, these approaches do not optimize a true lower bound of the ELBO (log evidence lower bound) for most of training. [32] proposes a modified objective to choose the model with the maximal rate (divergence). In [10] anti-causal sequential prior distributions are proposed with a lower bounded divergence for text modelling tasks. In contrast, [33] shows the advantage of normalizing flow based posteriors for preventing posterior collapse. In this work, we study for the first time the latent collapse problem in the context of flow based priors and propose a simple remedy which minimizes the true ELBO.

**Structured Sequence Prediction.** In this work we focus on traffic participant trajectories, particularly important for autonomous (assisted) driving. [34, 35, 36, 37, 38, 39] consider the problem of predicting trajectories of traffic participants in a social context. Notably, [37, 38] uses a generative adversarial network to generate socially compliant trajectories, this is further extended in [39]. However, the predictions are limited to being uni-modal. In [3, 2, 40, 41, 4] multi-modal (structured, one to many mappings) predictions are considered – [2] proposes an improved CVAE using the best of multiple samples during training, [40] learns pushforward policies for vehicle ego-motion prediction, [41] uses a motion planning based approach, [4] proposed a spatio-temporal convolutional network. Here, we focus on improving structured predictions using conditional normalizing flows based priors.

### 3 Conditional Flow Variational Autoencoders

Our Conditional Flow Variational Autoencoder is based on the conditional variational autoencoder [1] which is a deep directed graphical model for modeling conditional data distributions  $p_\theta(y|x)$ . CVAEs factorize conditional distributions using latent variables  $z$  which can be mapped to diverse predictions –  $p_\theta(y|x)$  is factorized as  $p_\theta(y|z, x)p(z|x)$ , where  $p(z|x)$  is the prior on the latent variables. During training, amortized variational inference is used and the posterior distribution of latent variables  $q_\phi(z|x, y)$  is learnt using a recognition network. The ELBO is maximized, given by,

$$\log(p_\theta(y|x)) \geq \mathbb{E}_{q_\phi(z|x, y)} \log(p_\theta(y|z, x)) - D_{\text{KL}}(q_\phi(z|x, y) || p(z|x)). \quad (1)$$

The KL divergence term on the right of (1) maintains the posterior distribution  $q_\phi(z|x, y)$  close to the prior. Low KL divergence to the prior is desirable as during inference we do not have access to the posterior distribution and thus we have to sample from the prior. In practice, to simplify learning, a simple unconditional standard Gaussian prior is used [1] ( $p(z|x)$  is set to  $p(z) = \mathcal{N}(0, I)$ ). But on complex conditional multi-modal data, standard Gaussian priors have been shown to induce a strong model bias resulting in missing modes and latent variable collapse [12]. This is due to two main disadvantages of unconditional standard Gaussian priors: 1. A standard Gaussian prior leads to simplistic posterior latent distributions which might not be sufficient to capture the multi-modal ground truth conditional distribution  $p(y|x)$ . In order to maintain the posteriors close to the prior, the model can choose to ignore modes and in extreme cases not encode any information in the latent distribution leading to collapse. 2. The ground truth conditional distribution  $p(y|x)$  can differ considerably depending upon the data point  $x$  e.g. the number of modes may vary depending upon  $x$  – a unconditional prior  $p(z)$  (however complex) cannot reflect this. Next, we describe how to tackle these shortcomings using complex multi-modal conditional flow based priors.

#### 3.1 Conditional Normalizing Flows

Recently, normalizing flow [42, 15] based priors for VAEs have been proposed [11, 12]. However, these flow based priors are unconditional. Here, we propose conditional priors instead of unconditional priors for integration into the CVAE framework, through the use of conditional normalizing flows. Our conditional normalizing flow based prior starts with a simple base distribution  $p(\epsilon|x)$ , which is then transformed by  $n$  layers of invertible normalizing flows  $f_i$ , with parameters  $\psi$ , to a more complex prior distribution (dependent on number of layers  $n$ ) on the latent variables  $p_\psi(z|x)$ ,

$$\epsilon|x \xrightarrow{f_1} h_1|x \xrightarrow{f_2} h_2|x \dots \xrightarrow{f_n} z|x. \quad (2)$$

Given the base density  $p(\epsilon|x)$  and the Jacobian  $J_i$  of each layer  $i$  of the transformation, the log-likelihood of the latent variable  $z$  can be expressed using the change of variables formula,

$$\log(p_\psi(z|x)) = \log(p(\epsilon|x)) + \sum_{i=1}^n \log(|\det J_i|). \quad (3)$$

We consider simple spherical Gaussians as base distributions,  $p(\epsilon|x) = \mathcal{N}(0, I)$  for efficient sampling (although more complex distributions are feasible). In contrast to prior work on conditional normalizing flows [20, 43, 44] which use affine flows, we build upon [12] and introduce conditional non-linear normalizing flows with split coupling. Split couplings ensure invertibility by applying a flow layer  $f_i$  on only half of the dimensions at a time. To compute (3), we split the dimensions  $z^D$  of

the latent variable into halfs,  $z^L = \{1, \dots, D/2\}$  and  $z^R = \{D/2, \dots, d\}$  at each invertible layer  $f_i$ . We then apply the following transformation each dimension  $z^j$  alternatively from  $z^L$  or  $z^R$ ,

$$f_i^{-1}(z^j | z^R, x) = \epsilon^j = a(z^R, x) + b(z^R, x) \times z^j + \frac{c(z^R, x)}{1 + (d(z^R, x) \times z^j + g(z^R, x))^2}. \quad (4)$$

where,  $z^j \in z^L$ . Details of the forward (generating) operation  $f_i$  are in Appendix A. Note that, in (4) and in the corresponding forward operation  $f_i$ , the coefficients  $\{a, b, c, d, g\} \in \mathbb{R}$  are functions of both the other half of the dimensions of  $z$  and the condition  $x$  (unlike [12]). Thus, the latent prior distribution on  $z$  is conditioned on  $x$ . Next, we describe our complete training objective.

### 3.2 Variational Inference using Conditional Normalizing Flows based Priors

Similar to CVAEs our approach also maximizes the ELBO (1). In case of the standard Gaussian prior, the KL divergence term has a simple closed form expression. In case of our conditional flow based prior, we can use the change of variables formula (3) to easily compute the KL divergence, by evaluating the likelihood over the base distribution instead of the complex conditional prior,

$$\begin{aligned} -D_{\text{KL}}(q_\phi(z|x, y) || p_\psi(z|x)) &= -\mathbb{E}_{q_\phi(z|x, y)} \log(q_\phi(z|x, y)) + \mathbb{E}_{q_\phi(z|x, y)} \log(p_\psi(z|x)) \\ &= \mathcal{H}(q_\phi) + \mathbb{E}_{q_\phi(z|x, y)} \log(p(\epsilon|x)) + \sum_{i=1}^n \log(|\det J_i|). \end{aligned} \quad (5)$$

where,  $\mathcal{H}(q_\phi)$  is the entropy of the variational distribution. Therefore, the ELBO can be expressed as,

$$\log(p_\theta(y|x)) \geq \mathbb{E}_{q_\phi(z|x, y)} \log(p_\theta(y|z, x)) + \mathcal{H}(q_\phi) + \mathbb{E}_{q_\phi(z|x, y)} \log(p(\epsilon|x)) + \sum_{i=1}^n \log(|\det J_i|) \quad (6)$$

To learn complex conditional priors, we jointly optimize both the variational posterior distribution  $q_\phi(z|x, y)$  and the conditional prior  $p_\psi(z|x)$  in (6) (akin to [7]). The variational posterior tries to match the conditional prior and vice-versa so that the ELBO (6) is maximized. We call this model the *Conditional Flow Variational Autoencoder (CF-VAE)*. Next, we discuss instabilities which might arise during training leading to latent variable collapse and corresponding solutions.

### 3.3 Dealing with Latent Variable Collapse

A frequently observed phenomenon in case of variational latent variable models is latent variable or posterior collapse [8, 9, 10]. In such cases, the latent variable does not encode any useful information. This happens when cost of encoding the data distribution into a meaningful latent distribution is greater than the cost of not explaining the data. We identify two potential causes of latent variable collapse in case of out conditional flow based CF-VAE and propose simple solutions for both.

The first cause is that in (6), the entropy and the log-Jacobian of the joint objective are at odds with each other. The log-Jacobian favours the contraction of the base density. Therefore, log-Jacobian at the right of (6) is maximized when the conditional flow maps the base distribution to a low entropy conditional prior (and thus a low entropy variational distribution  $q_\phi(z|x, y)$ ). Ideally, the CF-VAE should learn to balance these terms. However, in practice we observe instabilities during training. Degenerate solutions where either the entropy or the log-Jacobian terms dominate and the data log-likelihood is fully or partially ignored frequently emerge. To deal with this problem, we fix the variance of  $q_\phi(z|x, y)$  to  $C$ . In detail, we set  $q_\phi(z|x, y) = \mathcal{N}(\phi(x, y), C)$ . This results in a weaker posterior distribution but the entropy term becomes constant and no longer needs to be optimized. Moreover, the maximum possible amount of contraction also becomes bounded, thus upper bounding the log-Jacobian. Therefore, during training this encourages our model to concentrate on explaining the data and prevents degenerate solutions where either the entropy or the log-Jacobian terms dominate over the data log-likelihood, leading to more stable training and preventing latent variable collapse of our CF-VAE.

The second cause is the factorization of the conditional distribution used by our model,  $p_\theta(y|x) = p_\theta(y|z, x)p_\psi(z|x)$ . When the conditional data distribution has one or more minor modes, the condition  $x$  on the decoder might already be enough to model the main mode. If the cost of ignoring the minor

modes is out-weighed by the cost of encoding a complex latent distribution reflecting all modes, the CF-VAE might ignore the latent variables (set  $p_\theta(y|z, x) = p_\theta(y|x)$ ). We propose a simple solution – we remove the additional conditioning of the decoder on the condition  $x$ , when the dataset in question has minor modes. This assumes a simpler factorization of the conditional distribution  $p_\theta(y|x) = p_\theta(y|z)p_\psi(z|x)$ . This ensures that the latent variable  $z$  cannot be ignored by the CF-VAE and thus encodes useful information. Note that this assumption is only possible due to the fact that we learn a conditional prior, the Gaussian prior of the CVAE cannot encode conditional information.

### 3.4 Conditioning Priors on Contextual Information

In the following, we describe in detail how conditional flows (and thus our conditional priors  $p_\psi(z|x)$ ) can be conditioned on various contextual information e.g. past trajectories or environmental information, crucial to the accurate prediction of the future.

**Past Trajectory.** We encode the past trajectory using a LSTM to an fixed length vector  $x_t$ . For efficiency we share the condition encoder between the conditional flow and the CF-VAE decoder.

**Environmental Map.** We use a CNN to encode environmental information to a set of feature vectors. We apply a simple attention mechanism to extract a fixed length conditioning vector  $x_m$ .

**Interacting Traffic Participants/Agents.** To encode information of interacting traffic participants/agents, we use the convolutional social pooling of [45], where we exchange the LSTM trajectory encoder with  $1 \times 1$  convolutions for efficiency. In detail, convolutional social pooling [45] aggregates information using a grid overlayed on the environment. This grid is represented using a tensor, where the past trajectory information of traffic participants are aggregated into the tensor indexed corresponding to the grid in the environment. The past trajectory information is encoded using a LSTM before being aggregated into the grid tensor. For computational efficiency, we directly aggregate the trajectory information into the tensor, followed by a  $1 \times 1$  convolution to extract trajectory specific features. Finally, we apply several layers of  $k \times k$  convolutions to capture interaction aware contextual features  $x_p$  of traffic participants in the scene.

The conditional contextual information in finally aggregated into a single vector  $x = \{x_t, x_m, x_p\}$ . This vector is used as conditioning at every layer of our conditional non-linear flows  $f_i$  to condition our prior  $p_\psi(z|x)$ .

## 4 Experiments

We evaluate our CF-VAE on three popular and highly multi-modal sequence prediction datasets. In detail, given the sequence upto time  $t$ ,  $x = [x^1, \dots, x^t]$ , we predict the future sequence upto time  $T$ ,  $y = [y^{t+1}, \dots, y^T]$ . We begin with a description of our evaluation metrics and model architecture.

**Evaluation Metrics.** In line with prior work [3, 2, 4, 41, 46], we use metrics which measure fit to the groundtruth distribution. The negative conditional log-likelihood (-CLL) metric measures the likelihood of the ground-truth distribution under the learned model. Additionally, we report mean Euclidean distances of the oracle Top  $k\%$  of  $K$  predictions as in [3, 2, 4, 41]. This metric measures not only the coverage of all modes but also discourages random guessing for a reasonably large value of  $k$ . This is because, a model can improve its score by moving randomly guessed samples from an overestimated mode to the correct modes, such that for each test set example the Top  $k\%$  of predicted samples are closer. A value of  $k = 10\%$  is reasonably large to discourage random guessing in case of highly multi-modal datasets. We include a more detailed analysis in Appendix F.

**Conditional Flow Model Architecture.** Across all three datasets – MNIST Sequences [47], Stanford Drone [35] and HighD [48], we use the same conditional flow architecture with 16 layers of conditional non-linear flows with split coupling. Increasing the number of conditional non-linear flows generally led to “over-fitting” on the training latent distribution.

### 4.1 MNIST Sequence

The MNIST Sequence dataset [47] consists of sequences of handwriting strokes of the MNIST digits. We follow the evaluation protocol of [2] and predict the complete stroke given the first ten steps. The distribution of stroke completions is highly multi-modal and the number of modes varies considerably.

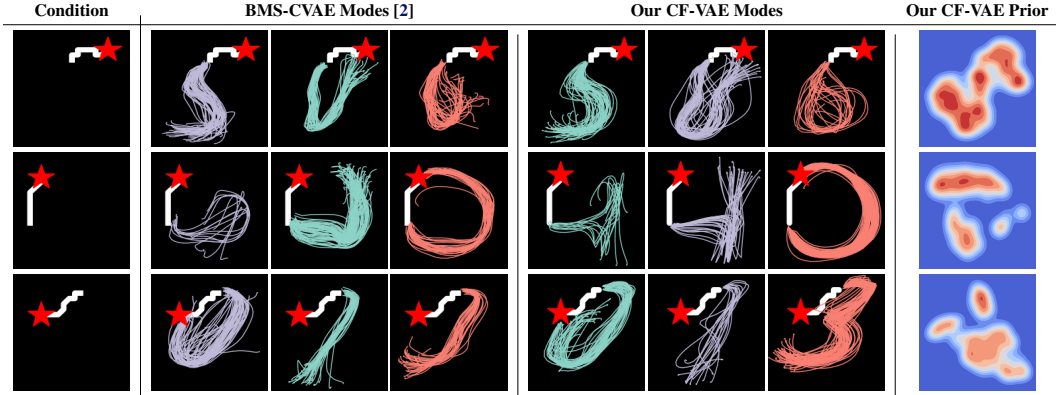


Figure 2: Random samples clustered using k-means. The number of clusters is set manually to the number of expected digits. The corresponding priors of our CF-VAE on the right. Note, our 64D CF-VAE latent distribution is (approximately) projected to 2D using tSNE and KDE.

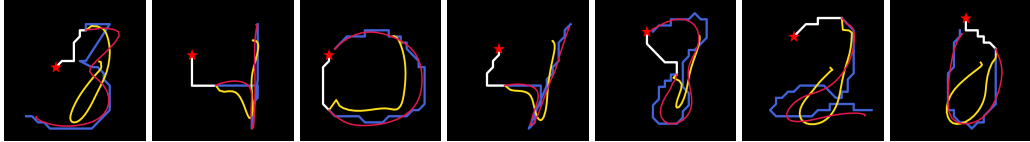


Figure 3: Comparing mean of top 10% of samples. Blue: Groundtruth, Yellow: BMS-CVAE [2], Magenta: Our CF-VAE. Our CF-VAE predictions are significantly closer to the groundtruth.

The state-of-the-art approach on this dataset is the CVAE based ‘‘Best-of-Many’’-CVAE [2]. Although constrained to a standard Gaussian prior, the BMS-CVAE uses multiple samples during training to help it capture multi-modal distributions. Additionally, we compare our CF-VAE with the following baselines: 1. A CVAE with a data dependent conditional mixture of Gaussians (MoG) prior; 2. A CF-VAE without a fixed variance variational posterior  $q_\phi(z|x, y)$ ; 3. A CF-VAE without the conditional non-linear flow layers (CF-VAE-CNL, replaced with affine coupling based flows [20, 43]). Note, although up to our knowledge, no prior work integrates MoG priors with CVAEs, we experiment with a conditional MoG prior for fairness (see Appendix D and E). We use the negative conditional log-likelihood (-CLL) metric for evaluation and the same model architecture across all baselines following [2] – LSTM encoders/decoders with 48 hidden neurons and a 64 dimensional latent space.

We report the results in Table 1. We see that our CF-VAE performs best. It has a performance advantage of over 20% against the state of the art BMS-CVAE. We further illustrate the modes captured and the learnt conditional flow based priors in Figure 2. For visualization, we project our conditional flow prior to 2D using tSNE followed by a kernel density estimate. We see that the number of modes in our conditional flow based prior  $p_\psi(z|x)$  reflects the number of modes in the data distribution  $p(y|x)$ . In contrast, the BMS-CVAE is unable to fully capture all modes – its predictions are pushed to the mean due to the strong model bias induced by the Gaussian prior. The results improve considerably with the multi-modal MoG prior ( $M = 3$  components work best). This highlights the need of a data-dependent multi-modal prior to capture the multi-modal distribution of handwriting strokes. Our CF-VAE still significantly outperforms the MoG-CVAE as normalizing flows are better at learning complex multi-modal distributions [17]. Next, we see that if we do not fix the variance ( $C = 0.2$ ) of the conditional posterior  $q_\phi(z|x, y)$ , there is latent collapse and a 40% drop in performance. This is because either the entropy or log-Jacobian term dominates during optimization. Moreover, note that our model is robust across a large range  $C = [0.05, 0.25]$  and thus tuning the hyper-parameter  $C$  is not challenging. We also see that using an affine conditional flow based prior leads to a drop in performance (77.2 vs 74.9

Method	-CLL
CVAE [1]	96.4
BMS-CVAE [2]	95.6
MoG-CVAE, $M = 3$	84.6
CF-VAE - CNL layers	77.2
CF-VAE - fixed variance $q_\phi$	104.3
CF-VAE (Ours)	<b>74.9</b>

Table 1: Evaluation on MNIST Sequences (CLL: lower is better).

Method	Visual	Error @ 1sec	Error @ 2sec	Error @ 3sec	Error @ 4sec	CLL
“Shotgun” (Top 10%) [4]	None	0.7	1.7	3.0	4.5	91.6
DESIRE-SI-IT4 (Top 10%) [3]	RGB	1.2	2.3	3.4	5.3	x
STCNN (Top 10%) [4]	RGB	1.2	2.1	3.3	4.6	x
BMS-CVAE (Top 10%) [2]	RGB	0.8	1.7	3.1	4.6	126.6
MoG-CVAE, $M = 3$ (Top 10%)	None	0.8	1.7	2.7	3.9	86.1
CF-VAE (Ours, Top 10%)	None	<b>0.7</b>	<b>1.5</b>	2.5	3.6	84.6
CF-VAE (Ours, Top 10%)	RGB	<b>0.7</b>	<b>1.5</b>	<b>2.4</b>	<b>3.5</b>	<b>84.1</b>

Table 2: Five fold cross validation on the Stanford Drone dataset. Euclidean error at  $(1/5)$  resolution.

CLL). This further illustrates the advantage of our non-linear conditional flows in learning highly non-linear priors.

## 4.2 Stanford Drone

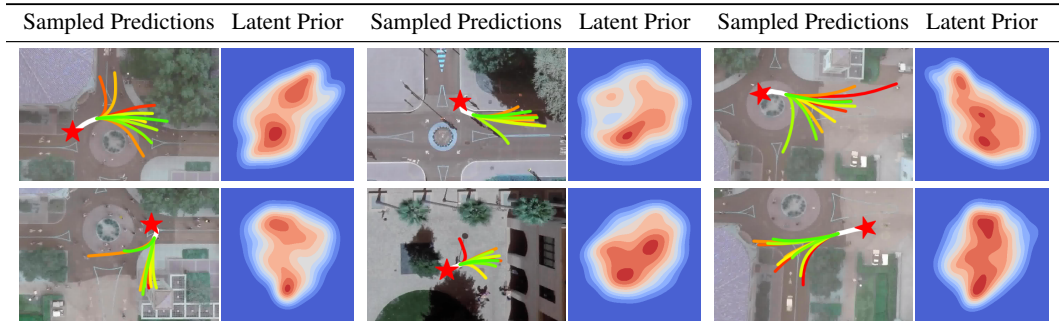


Figure 4: Randomly sampled predictions of our CF-VAE model on the Stanford Drone dataset. We observe that our prediction are highly multi-modal and is reflected by the Conditional Flow Priors. Note, our 64D CF-VAE latent distribution is (approximately) projected to 2D using tSNE and KDE.



Figure 5: Comparison of our CF-VAE (Red) versus the “Shotgun” baseline (Yellow) of [4], Groundtruth (Blue). Initial conditioning trajectory in white. Our CF-VAE not only learns to capture the correct modes but also generates more fine-grained predictions.

The Stanford Drone dataset [35] consists of trajectories of traffic participant e.g. pedestrians, bicyclists, cars in videos captured from a drone. The scenes are dense in traffic participants with highly multi-modal trajectories. Prior work follows two different evaluation protocols, 1. [3, 2, 4] use 5 fold cross validation, 2. [35, 49, 39, 41] use a single standard train-test split. We evaluate our CF-VAE using the first protocol in Table 2 and the second in Table 3.

In addition to these state of the art models, [4] suggests a “Shotgun” baseline. This baseline extrapolates the trajectory from the last known position and orientation in 10 different ways – 5 orientations:  $(0^\circ, \pm 8^\circ, \pm 15^\circ)$  and 5 velocities: None or exponentially weighted over the past with coefficients  $(0, 0.3, 0.7, 1.0)$ . This baseline obtains results at par with the state-of-the-art because it a good template which covers the most likely possible futures (modes) for traffic participant motion in this dataset. We report the results using 5 fold cross validation in Table 2. We additionally compare to a mixture of Gaussians prior (details

Method	mADE	mFDE
SocialGAN [37]	27.2	41.4
MATF GAN [38]	22.5	33.5
SoPhie [39]	16.2	29.3
Goal Prediction [41]	15.7	28.1
CF-VAE (Ours)	<b>12.6</b>	<b>22.3</b>

Table 3: Evaluation on the Stanford Drone dataset using the split of [37, 38, 39, 41] (see also Table 2).

in Appendix D). We use the same model architecture as in [2] and a CNN encoder with attention to extract features from the last observed RGB image (details in Appendix C). These visual features serve as additional conditioning ( $x_m$ ) to our Conditional Flow model. We see that our CF-VAE model with RGB input and  $C = 0.2$  performs best – outperforming the state-of-art “Shotgun” and BMS-CVAE by over 20% (Error @ 4sec). We see that our conditional flows are able to utilize visual scene (RGB) information to improve performance (3.5 vs 3.6 Error @ 4sec). We also see that the MoG-CVAE and our CF-VAE outperform the BMS-CVAE, even without visual scene information. This again reinforces our claim that the standard Gaussian prior induces a strong model bias and data dependent multi-modal priors are needed for best performance. The performance advantage of CF-VAE over the MoG-CVAE again illustrates the advantage of normalizing flows at learning complex conditional multi-modal distributions. The performance advantage over the “Shotgun” baseline shows that our CF-VAE not only learns to capture the correct modes but also generates more fine-grained predictions. The qualitative examples in Figure 5 shows that our CF-VAE is better able to capture complex trajectories with sharp turns.

We report results using the single train/test split of [35, 49, 39, 41] in Table 3. We use the minimum Average Displacement Error (mADE) and minimum Final Displacement Error (mFDE) metrics as in [41]. The minimum is over a set of predictions of size  $K$ . Although this metric is less robust to random guessing compared to the Top  $k\%$  metric, it avoids rewarding random guessing for a small enough value of  $K$ . We choose  $K = 20$  as in [41]. Similar to the results with 5 fold cross validation, we observe 20% improvement over the state-of-the-art.

### 4.3 HighD

The HighD dataset [48] consists of vehicle trajectories recorded using a drone over highways. In contrast to other vehicle trajectory datasets e.g. NGSIM it contains minimal false positive trajectory collisions or physically improvable velocities. Therefore, it does not require additional filtering and smoothing which otherwise makes results unreliable.

However, the HighD dataset is challenging because only 10% of the vehicle trajectories contain a lane change or interaction – the conditional distributions contain a single main mode along with several minor modes. Thus, approaches which predict a single mean trajectory (targeting the main mode) are challenging to outperform. In Table 4, we see that the simple Feed Forward (FF) model performs well and the Graph Convolutional GAT model of [50], which

Method	Context	ADE	FDE	-CLL
Constant Velocity	None	1.09	2.66	x
FF [50]	None	0.45	1.09	x
GAT [50]	Yes	0.47	1.04	x
CVAE (Top 10%)	None	0.38	0.80	4.80
CF-VAE (Ours, Top 10%)	None	0.30	0.57	3.64
CF-VAE (Ours, Top 10%)	Yes	<b>0.29</b>	<b>0.55</b>	<b>3.42</b>

Table 4: Evaluation on the HighD dataset.

captures interactions, only narrowly outperforms the FF model. This dataset is challenging for CVAE based models as they frequently suffer from posterior collapse when a single mode dominates. This is clearly observed with our CVAE baseline in Table 4. To prevent complete posterior collapse, we use the cyclic KL annealing scheme proposed in [31] (using a MoG prior did not help here). This already leads to significant improvement over the deterministic FF and GAT baselines. We also observe posterior collapse with our CF-VAE model. Therefore, we use the simple strategy of removing the additional conditioning of the past trajectory from the decoder (see subsection 3.3). Our plain CF-VAE ( $C = 0.1$ ) significantly outperforms the CVAE baseline (with cyclic KL annealing), demonstrating that posterior collapse not occur. The addition of contextual information of interacting traffic participants improves performance (also see Appendix G). This demonstrates that our conditional non-linear Flows can effectively learn complex priors to even capture minor modes.

## 5 Conclusion

In this work, we presented the first novel variational model for learning multi-modal conditional data distributions with Conditional Flow based priors – the Conditional Flow Variational Autoencoder. Our rigorous experiments on diverse sequence prediction datasets show that our CF-VAE achieves state-of-the-art results. Furthermore, we address latent variable collapse using fixed variance posteriors and removing additional conditioning information from the decoder. Additionally, we also show that our powerful Conditional Flow Variational Autoencoder can take advantage of diverse sources of conditioning information including scene context and interacting agents.

## References

- [1] K. Sohn, H. Lee, and X. Yan. Learning structured output representation using deep conditional generative models. In *NIPS*, 2015.
- [2] A. Bhattacharyya, B. Schiele, and M. Fritz. Accurate and diverse sampling of sequences based on a best of many sample objective. In *CVPR*, 2018.
- [3] N. Lee, W. Choi, P. Vernaza, C. B. Choy, P. H. Torr, and M. Chandraker. Desire: Distant future prediction in dynamic scenes with interacting agents. In *CVPR*, 2017.
- [4] E. Pajouheshgar and C. H. Lampert. Back to square one: probabilistic trajectory forecasting without bells and whistles. In *NeurIPS Workshop*, 2018.
- [5] M. Babaeizadeh, C. Finn, D. Erhan, R. H. Campbell, and S. Levine. Stochastic variational video prediction. In *ICLR*, 2018.
- [6] M. D. Hoffman and M. J. Johnson. Elbo surgery: yet another way to carve up the variational evidence lower bound. In *NIPS Workshop*, 2016.
- [7] J. M. Tomczak and M. Welling. Vae with a vampprior. In *AISTATS*, 2018.
- [8] S. R. Bowman, L. Vilnis, O. Vinyals, A. M. Dai, R. Jozefowicz, and S. Bengio. Generating sentences from a continuous space. *CONLL*, 2016.
- [9] I. Higgins, L. Matthey, A. Pal, C. Burgess, X. Glorot, M. Botvinick, S. Mohamed, and A. Lerchner. beta-vae: Learning basic visual concepts with a constrained variational framework. In *ICLR*, 2017.
- [10] A. Razavi, A. v. d. Oord, B. Poole, and O. Vinyals. Preventing posterior collapse with delta-vae. In *ICLR*, 2019.
- [11] X. Chen, D. P. Kingma, T. Salimans, Y. Duan, P. Dhariwal, J. Schulman, I. Sutskever, and P. Abbeel. Variational lossy autoencoder. In *ICLR*, 2017.
- [12] Z. M. Ziegler and A. M. Rush. Latent normalizing flows for discrete sequences. In *ICML*, 2019.
- [13] L. v. d. Maaten and G. Hinton. Visualizing data using t-sne. In *JMLR*, 2008.
- [14] B. W. Silverman. *Density estimation for statistics and data analysis*. Routledge, 2018.
- [15] L. Dinh, D. Krueger, and Y. Bengio. Nice: Non-linear independent components estimation. In *ICLR*, 2015.
- [16] L. Dinh, J. Sohl-Dickstein, and S. Bengio. Density estimation using real nvp. In *ICLR*, 2017.
- [17] D. P. Kingma and P. Dhariwal. Glow: Generative flow with invertible 1x1 convolutions. In *NeurIPS*, 2018.
- [18] C.-W. Huang, D. Krueger, A. Lacoste, and A. Courville. Neural autoregressive flows. In *ICML*, 2018.
- [19] J. Behrmann, D. Duvenaud, and J.-H. Jacobsen. Invertible residual networks. In *ICML*, 2019.
- [20] Y. Lu and B. Huang. Structured output learning with conditional generative flows. In *ICML Workshop*, 2019.
- [21] D. P. Kingma and M. Welling. Auto-encoding variational bayes. In *ICLR*, 2014.
- [22] D. J. Rezende and S. Mohamed. Variational inference with normalizing flows. In *ICML*, 2015.
- [23] D. P. Kingma, T. Salimans, R. Jozefowicz, X. Chen, I. Sutskever, and M. Welling. Improved variational inference with inverse autoregressive flow. In *NIPS*, 2016.
- [24] J. M. Tomczak and M. Welling. Improving variational auto-encoders using householder flow. In *NIPS Workshop*, 2016.
- [25] R. v. d. Berg, L. Hasenclever, J. M. Tomczak, and M. Welling. Sylvester normalizing flows for variational inference. In *UAI*, 2018.
- [26] E. Nalisnick and P. Smyth. Stick-breaking variational autoencoders. In *ICLR*, 2017.
- [27] P. Goyal, Z. Hu, X. Liang, C. Wang, and E. P. Xing. Nonparametric variational auto-encoders for hierarchical representation learning. In *ICCV*, 2017.

[28] Z. Yang, Z. Hu, R. Salakhutdinov, and T. Berg-Kirkpatrick. Improved variational autoencoders for text modeling using dilated convolutions. In *ICML*, 2017.

[29] A. B. Dieng, Y. Kim, A. M. Rush, and D. M. Blei. Avoiding latent variable collapse with generative skip models. *AISTATS*, 2019.

[30] I. Gulrajani, K. Kumar, F. Ahmed, A. A. Taiga, F. Visin, D. Vazquez, and A. Courville. Pixelvae: A latent variable model for natural images. In *ICLR*, 2017.

[31] X. Liu, J. Gao, A. Celikyilmaz, L. Carin, et al. Cyclical annealing schedule: A simple approach to mitigating kl vanishing. In *NAACL*, 2019.

[32] S. Zhao, J. Song, and S. Ermon. Infovae: Information maximizing variational autoencoders. In *arXiv preprint arXiv:1706.02262*, 2017.

[33] P. Z. Wang and W. Y. Wang. Riemannian normalizing flow on variational wasserstein autoencoder for text modeling. In *NAACL*, 2019.

[34] D. Helbing and P. Molnar. Social force model for pedestrian dynamics. *Physical review E*, 51, 1995.

[35] A. Robicquet, A. Sadeghian, A. Alahi, and S. Savarese. Learning social etiquette: Human trajectory understanding in crowded scenes. In *ECCV*, 2016.

[36] A. Alahi, K. Goel, V. Ramanathan, A. Robicquet, L. Fei-Fei, and S. Savarese. Social lstm: Human trajectory prediction in crowded spaces. In *CVPR*, 2016.

[37] A. Gupta, J. Johnson, L. Fei-Fei, S. Savarese, and A. Alahi. Social gan: Socially acceptable trajectories with generative adversarial networks. In *CVPR*, 2018.

[38] T. Zhao, Y. Xu, M. Monfort, W. Choi, C. Baker, Y. Zhao, Y. Wang, and Y. Nian Wu. Multi-agent tensor fusion for contextual trajectory prediction. In *CVPR*, 2019.

[39] A. Sadeghian, V. Kosaraju, A. Sadeghian, N. Hirose, S. H. Rezatofighi, and S. Savarese. Sophie: An attentive gan for predicting paths compliant to social and physical constraints. In *CVPR*, 2019.

[40] N. Rhinehart, K. M. Kitani, and P. Vernaza. R2p2: A reparameterized pushforward policy for diverse, precise generative path forecasting. In *ECCV*, 2018.

[41] N. Deo and M. M. Trivedi. Scene induced multi-modal trajectory forecasting via planning. In *ICRA Workshop*, 2019.

[42] E. G. Tabak, E. Vanden-Eijnden, et al. Density estimation by dual ascent of the log-likelihood. In *Communications in Mathematical Sciences*, volume 8, 2010.

[43] A. Atanov, A. Volokhova, A. Ashukha, I. Sosnovik, and D. Vetrov. Semi-conditional normalizing flows for semi-supervised learning. In *ICML Workshop*, 2019.

[44] L. Ardizzone, J. Kruse, S. Wirkert, D. Rahner, E. W. Pellegrini, R. S. Klessen, L. Maier-Hein, C. Rother, and U. Köthe. Analyzing inverse problems with invertible neural networks. In *ICLR*, 2019.

[45] N. Deo and M. M. Trivedi. Convolutional social pooling for vehicle trajectory prediction. In *CVPR Workshop*, 2018.

[46] A. Bhattacharyya, M. Fritz, and B. Schiele. Bayesian prediction of future street scenes using synthetic likelihoods. In *ICLR*, 2019.

[47] E. D. De Jong. The mnist sequence dataset. <https://edwin-de-jong.github.io/blog/mnist-sequence-data/>, 2016. Accessed: 2019-07-07.

[48] R. Krajewski, J. Bock, L. Kloeker, and L. Eckstein. The highd dataset: A drone dataset of naturalistic vehicle trajectories on german highways for validation of highly automated driving systems. In *ITSC*, 2018.

[49] A. Sadeghian, F. Legros, M. Voisin, R. Vesel, A. Alahi, and S. Savarese. Car-net: Clairvoyant attentive recurrent network. In *ECCV*, 2018.

[50] F. Diehl, T. Brunner, M. T. Le, and A. Knoll. Graph neural networks for modelling traffic participant interaction. In *ITSC*, 2019.

[51] G. Holmes. The use of hyperbolic cosines in solving cubic polynomials. *The Mathematical Gazette*.

## Appendix A. Conditional Non-Linear Normalizing Flows

In Subsection 3.1 of the main paper, we describe the inverse operation  $f_i^{-1}$  of our non-linear conditional normalizing flows. Here, we describe the forward operation. Note that while the forward operation is necessary to compute the likelihood (3) (in the main paper) during training, the forward operation is necessary to sample from the latent prior distribution of our CF-VAE. The forward operation consists of solving for the roots of the following equation (more details in [12]),

$$\begin{aligned} & -bd^2(\epsilon^j)^3 + ((z^j - a)d^2 - 2dgb)(\epsilon^j)^2 \\ & + (2dg(z^j - a) - b(g^2 + 1))\epsilon^j + ((z^j - a)(g^2 + 1) - c) = 0 \end{aligned} \quad (7)$$

This equation has one real root which can be found analytically [51]. As mentioned in the main paper, note that the coefficients  $\{a, b, c, d, g\}$  are also functions of the condition  $x$  (unlike [12]).

## Appendix B. Additional Evaluation of Conditional Non-Linear Flows

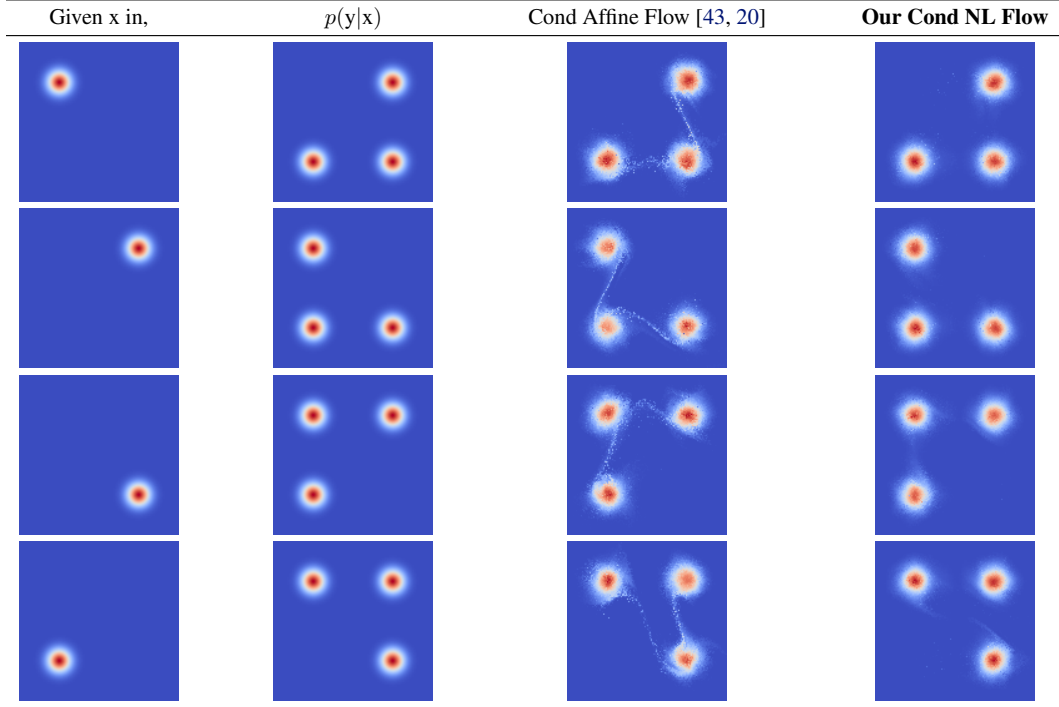


Figure 6: Comparison between conditional affine flows of [43, 20] and our conditional non-linear (Cond NL) flows. We see that the conditional affine flows cannot fully capture multi-modal distributions (“tails” between modes), while our conditional non-linear flows does not have distinctive “tails”.

We compare conditional affine flows of [43, 20] and our conditional non-linear (Cond NL) flows in Figure 6 and Figure 7. We plot the conditional distribution  $p(y|x)$  and the corresponding condition  $x$  in the second and first columns. We use 8 and 16 layers of flow in case of the densities in Figure 6 and Figure 7 respectively. We see that the estimated density by the conditional affine flows of [43, 20] contains distinctive “tails” in case of Figure 6 and discontinuities in case of Figure 7. In comparison our conditional non-linear flows does not have distinctive “tails” or discontinuities and is able to complex capture the multi-modal distributions better. Note, the “ring”-like distributions in Figure 7 cannot be well captured by more traditional methods like Mixture of Gaussians. We see in Figure 8 that even with 64 mixture components, the learnt density is not smooth in comparison to our conditional non-linear flows. This again demonstrates the advantage of our conditional non-linear flows.

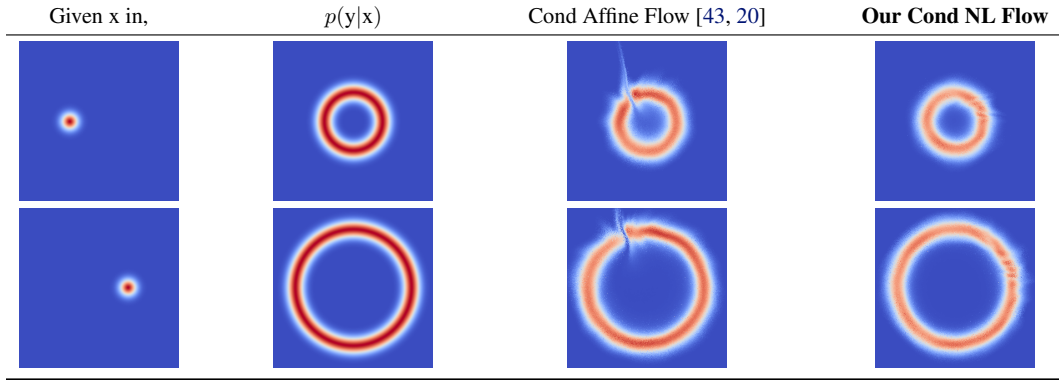


Figure 7: Comparison between conditional affine flows of [43, 20] and our conditional non-linear (Cond NL) flows. We see that the conditional affine flows cannot fully capture “ring”-like conditional distributions (note the discontinuity at the top), while our conditional non-linear flows does not have such discontinuities.

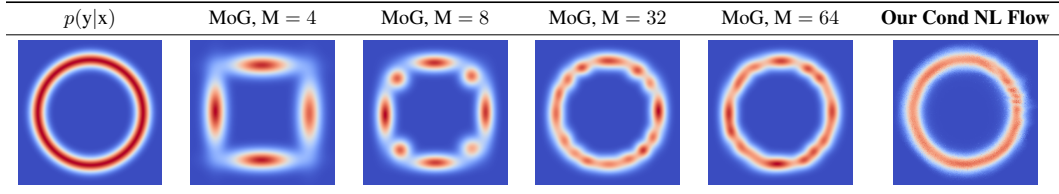


Figure 8: Comparison between our conditional non-linear (Cond NL) flows and a Mixture of Gaussians (MoG) model. We see that even with 64 mixture components, the learnt density is not smooth in comparison to our conditional non-linear flows.

## Appendix C. Additional Details of Our Model Architectures

Here, we provide details of the model architectures used across the three datasets used in the main paper.

**MNIST Sequences.** We use the same model architecture as in [2]. The LSTM condition encoder on the input sequence  $x$ , the LSTM recognition network  $q_\theta$  and the decoder LSTM network has 48 hidden neurons each. Also as in [2], we use a 64 dimensional latent space.

**Stanford Drone.** Again, we use the same model architecture as in [2] except for the CNN encoder. The LSTM condition encoder on the input sequence  $x$  and the decoder LSTM network has 64 hidden neurons each. The LSTM recognition network  $q_\theta$  has 128 hidden neurons. Also as in [2], we use a 64 dimensional latent space. Our CNN encoder has 6 convolutional layers of size 32, 64, 128, 256, 512 and 512. We predict the attention weights on the final feature vectors using the encoding of the LSTM condition encoder. The attention weighted feature vectors are passed through a final fully connected layer to obtain the final CNN encoding. Furthermore, we found it helpful to additionally encode the past trajectory as an image (as in [4]) as provide this as an additional channel to the CNN encoder.

**HighD.** We use the same model architecture with both the CVAE and CF-VAE models. As in the Stanford drone dataset, we use LSTM condition encoder on the input sequence  $x$  and the decoder LSTM network with 64 hidden neurons each and the LSTM recognition network  $q_\theta$  with 128 hidden neurons. The contextual information of interacting traffic participants are encoded into a spatial grid tensor of size  $13 \times 3$  (see Section 3.4 of the main paper). We use a CNN with 5 layers of sizes 64, 128, 256, 256 and 256 to extract contextual features.

## Appendix D. Details of the mixture of Gaussians (MoG) baseline

In the main paper, we include results on the MNIST Sequence and Stanford Drone dataset with a Mixture of Gaussians (MoG) prior. Although such priors have been proposed for plain VAEs [7], upto our knowledge there are no prior works which integrate MoG priors with CVAEs. However, for fairness we experiment with a conditional MoG prior. In detail, instead of a normalizing flow, we set the prior to a MoG form,

$$p_\xi(z|x) = \sum_{i=1}^M p(c_i|x) \mathcal{N}(z; \mu_i, \sigma_i|x). \quad (8)$$

We use a simple feed forward neural network that takes in the condition  $x$  (see Section 3.4 of the main paper) and predicts the parameters of the MoG,  $\xi = \{c_1, \mu_1, \sigma_1, \dots, c_M, \mu_M, \sigma_M\}$ . Note, to ensure a reasonable number of parameters, we consider spherical Gaussians. Similar to (5) in the main paper, the ELBO can be expressed as,

$$\log(p_\theta(y|x)) \geq \mathbb{E}_{q_\phi(z|x,y)} \log(p_\theta(y|z,x)) + \mathcal{H}(q_\phi) + \mathbb{E}_{q_\phi(z|x,y)} \log(p_\xi(z|x)). \quad (9)$$

Note that we fix the entropy of the posterior distribution  $q_\phi$  to prevent latent collapse.

## Appendix E. Additional Evaluation on the MNIST Sequence Dataset

Here, we perform a comprehensive evaluation using the MoG prior with varying mixture components. Moreover, we experiment with a CVAE with unconditional non-linear flow based prior (NL-CVAE). We report the results in [Table 5](#).

Method	-CLL
NL-CVAE	107.6
CVAE ( $M = 1$ ) [1]	96.4
MoG-CVAE, $M = 2$	85.3
MoG-CVAE, $M = 3$	84.6
MoG-CVAE, $M = 4$	85.7
MoG-CVAE, $M = 5$	86.3
CF-VAE	<b>74.9</b>

Table 5: Evaluation on MNIST Sequences (CLL: lower is better).

As mentioned in the main paper, we see that the MoG-CVAE outperforms the plain CVAE. This again reinforces our claim that the standard Gaussian prior induces a strong model bias. We see that using  $M = 3$  components with the variance of the posterior distribution fixed to  $C = 0.2$  (to avoid latent collapse) leads to the best performance. This is expected as 3 is the most frequent number of possible strokes in the MNIST Sequence dataset. Also note that the results with the MoG prior are also relatively robust across  $C = [0.05, 0.2]$  as we learn the variance of the prior (see the section above). Finally, our CF-VAE still significantly outperforms the MoG-CVAE (74.9 vs 84.6). This is expected as normalizing flows are more powerful compared to MoG at learning complex multi-modal distributions [17] (also see [Figure 8](#)).

We also see that using an unconditional non-linear flow based prior actually harms performance (107.6 vs 96.4). This is because the latent distribution is highly dependent upon the condition. Therefore, without conditioning information the non-linear conditional flow learns a global representation of the latent space which leads to out-of-distribution samples at prediction time.

## Appendix F. Evaluation of the Robustness of the Top k% Metric

We use two simpler uniform ‘‘Shotgun’’ baselines to study the robustness of the Top k% metric against random guessing. In particular, we consider the ‘‘Shotgun’’-u90° and ‘‘Shotgun’’-u135° baselines

which: given a budget of  $K$  predictions, it uniformly distributes the predictions between  $(-90^\circ, 90^\circ)$  and  $(-135^\circ, 135^\circ)$  respectively of the original orientation and using the velocity of the last time-step. In [Table 6](#) we compare the Top 1 (best guess) to Top 10% metric with  $K = 50, 100, 500$  predictions.

Method	K	Error @ 1sec	Error @ 2sec	Error @ 3sec	Error @ 4sec
Top 1 (Best Guess)					
“Shotgun”-u90°	50	0.9	1.9	3.1	4.4
“Shotgun”-u90°	100	0.9	1.9	3.0	4.3
“Shotgun”-u90°	500	0.9	1.9	3.0	4.3
Top 10%					
“Shotgun”-u90°	50	1.2	2.5	3.9	5.4
“Shotgun”-u90°	100	1.2	2.5	3.9	5.4
“Shotgun”-u90°	500	1.2	2.5	3.9	5.4
Top 1 (Best Guess)					
“Shotgun”-u135°	50	0.9	2.0	3.1	4.5
“Shotgun”-u135°	100	0.9	1.9	3.0	4.3
“Shotgun”-u135°	500	0.9	1.9	3.0	4.2
Top 10%					
“Shotgun”-u135°	50	1.4	2.9	4.5	6.2
“Shotgun”-u135°	100	1.4	2.9	4.5	6.2
“Shotgun”-u135°	500	1.4	2.9	4.5	6.2

Table 6: Five fold cross validation on the Stanford Drone dataset. Euclidean error at  $(1/5)$  resolution.

We see that in case of both the “Shotgun”-u90° and “Shotgun”-u135° baselines, the Top 1 (best guess) metric improves with increasing number of guesses. This effect is even more pronounced in case of the “Shotgun”-u135° baseline as the random guesses are distributed over a larger spatial range. In contrast, the Top 10% metric remains remarkably stable. This is because, in order to improve the Top 10% metric, random guessing is not enough – the predictions have to be on the correct modes. In other words, the only way to improve the Top 10% metric is move random predictions to any of the correct modes.

## Appendix G. Qualitative Examples on the HighD Dataset

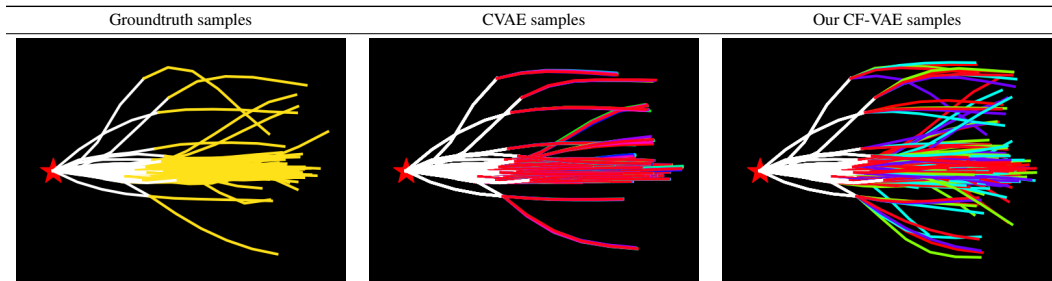


Figure 9: Predictions on the HighD dataset. Left: 128 random samples from the HighD test set (in yellow). Middle: CVAE predictions (5 samples per test set example). Right: Our CF-VAE predictions (5 samples per test set example). While the predictions by the CVAE are linear continuations, our CF-VAE sample predictions are much more diverse and cover events like lane changes e.g. top most sample track from the test set.

We show qualitative examples on the HighD dataset in [Figure 9](#). In the left of [Figure 9](#) we show 128 random samples from the HighD test set. In the middle we show predictions on these samples by

the CVAE (with cyclic KL annealing [31]). We see that even with cyclic KL annealing, we observe partial latent collapse. All samples have been pushed towards the mean and the variance in the 5 samples per test set example is minimal. E.g. note the top most sample track from the test set in Figure 9 (left). All CVAE sample predictions are a linear continuation of the trajectory (continuing on the same lane), while there is in fact a turn (change of lanes). In contrast, our CF-VAE sample predictions are much more diverse and cover such eventualities. This also shows that our CF-VAE does not suffer from such latent variable collapse.